Feedforward Control for Polymer Laser Sintering Process Using Part Geometry

Mostafa Abdelrahman* and Thomas L. Starr**

*Rapid Prototyping Center, **Chemical Engineering Department,
J.B. Speed School of Engineering, University of Louisville, Louisville, KY 40292

REVIEWED

Abstract

For the polymer laser sintering process, achieving optimum mechanical properties requires that every volume element of a part experience a temperature history sufficient to reach full density. This history must include a peak temperature high enough to fully melt, but not degrade, the polymer and a cool-down period that ensures elimination of porosity, interlayer bonding and relaxation of stress. Real-time thermal monitoring of the laser sintering process has shown that this temperature history depends on the geometries of both the current and prior layers. In this paper we demonstrate a feed-forward control system that improves uniformity of the temperature history for parts with variable cross-sections. The control algorithm for this system will utilize information from layerwise geometry models for parts in a multi-part build. The cross-sectional area for every layer will be used at run-time for feed forward control the laser scan parameters. The results confirmed maintaining constant peak temperature throughout the part. This control system ensures optimized sintering for parts with complex geometries.

Introduction

Polymer laser sintering is an additive manufacturing method that converts layers of polymer powder into a dense 3D structure by selectively heating areas with a scanning laser. While this technology was developed more than 30 years ago all commercial machines operate with open loop control and limited monitoring and control of the process. Temperature control is a critical problem for the sintering of polymer powders. Achieving optimum mechanical properties requires that every volume element of a part experience a temperature history sufficient to reach full density. Process monitoring and control can be used to certify that a process is running consistently and within specifications for a particular material and process. A set of parameters can be determined to be controlled during the fabrication process. Examples of these parameters include the powder bed temperature and the peak temperature during the scan. Controlling this parameter set can establish the range of parameter values that produce "good" parts. Information from layerwise geometry models for parts can be used to control the process parameters. These geometric information can be used to adjust the laser beam power and other scan parameters.

Previous investigators used optical sensors for laser sintering process monitoring, [1, 2, 3, 4,5,6]. All of this work analyses the optical emission results from the melt process in one or more spectral ranges. Diller et. al. [7] proposed to use thermal imaging for monitoring the laser sintering process. They proposed to analyse the temperature distribution on the part bed surface. Thermal imaging systems have been integrated into the Laser Sintering systems to monitor the thermal history, correlate the outcomes, and plan an optimized approach for part manufacture in [8, 9, 10,11]. However, these methods do not provide a quality certification of the process, and do not suggest how to use the monitor data to provide control signals for the sintering process.

A new control method that takes advantage of the unique characteristics of the layerwise AM processes is needed. This method will use process control techniques to maintain the optimum process parameters. These control signals will maintain a uniform temperature distribution of the powder bed surface in order to achieve equal part quality. The control signals may depend on the geometry of the layers and the process history of previous layers. One of the most important parameters that can be used to control the process is the cross section area of the layers. Our previuos work about the 3D indexing [12], with the proposed control signals will enable: setting up optimal laser beam parameters prior to the manufacturing process, controlling laser beam parameters during the manufacturing process, controlling the wait time before adding powder for the next layer, inspecting the quality of the current layer online, and creating a 3D Quality Certificate for the part being built.

Process Control Systems

Process control systems can be classified generally as open-loop, feed-forward or feed-back (closed-loop). Current commercial polymer LS equipment employs some elements of each control method. Normally a "set point" for laser power is determined prior to the start of the build and this output is maintained throughout the build period. This open-loop control corresponds to no "sensor" or "disturbance" inputs in Figure 1. Although rarely used, current LS software from 3D Systems does have a provision for changing laser power as a function of build height. Build height would be a "disturbance" in Figure 1 and it would feed forward to the change the output laser power. The powder bed heater subsystem in current LS machines employs a simple closed-loop control method. A pyrometer measures the temperature at a point on the powder bed surface. This "sensor" signal is fed back and compared to the "setpoint" value and the difference is use to control the heater power. By design this system can only control temperature at one point on powder bed surface and has no provision for incorporating feed-forward information about layer geometry.

The shortcomings of current commercial LS control systems lead to unacceptable variability in material properties, as discussed above. The improved polymer LS process control system proposed here will include elements both of open and closed loop process control. Scan and temperature parameters will be set prior to the build but can be adjusted layer-by-layer based on the part and packing geometry of the layer (disturbance) and on real-time temperature measurements (sensor). Layerwise thermal imaging data will provide a richer set of monitor information that can be fed back to the control system. Control models (G's) will be designed in future work to convert these inputs into control signals.
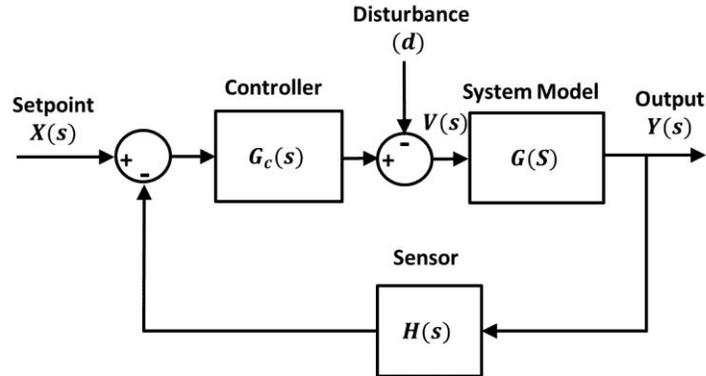
Figure 1. Process control can be achieved using a combination of feedforward and feedback methods. Models (G's) are used to convert inputs into control signals.

In our previous work in [14], we show that there is a relationship between the peak temperature value and the geometry of the part, the layer cross-sectional area, and the presence or absence of an underlying solid layer. We aproved that control signals can be generated to control the fabrication of the next layer and the wait time before adding the powder for the next layer. And we show that the cross section area can be used as a control signal to control the laser scan parameters. In this paper we propose to use the layer cross-sectional area to control the laser beam power in order to maintain a uniform peak temperature inside the build volume.

Data Collection

Fig. 3 shows the experiment setup. The system consists of a new open architecture polymer LS machine, thermal camera, 2 in flat gold mirror, and a computer. The process is monitored by a FLIR SC7000 MWIR thermal camera. The thermal camera is mounted as shown in Fig. 3 to view the building bed through the top laser window. The laser window and the mirror have a transmittance equal to 53% in the camera's wavelenth range. The camera is focused manually on the region where the part will be built. For this experiment, a 50 mm focal length lens is used and the frame rate set to 100 fps with window size of 255x175. The SLS machine takes about 230 minutes to build the one of the test parts. One SAF video is recorded for every part build. Every recorded video size is about 100 GB.

Data Analysis

The raw intensity data is mapped to the real temperature values using a 1st-order mapping function. The transmittance is set to 53% to compensate for the laser window and the mirror attenuation. The frames are parsed into individual layers using the using the maximum temperature in each frame as a marker as described in [12]. We selected 100 frame during the scan time for every layer. For each set of 100 frames the peak temperature value is detected for each point in the window area. These peak temperature values are assembled to form a single image for each layer. These images will be used to studey the effect of changing the laser beam power as a function in the cross-sectional area.

Figure 2. System setup consists of the new "open architecture" LS machine, thermal camera and a 2 in flat gold mirror.

Template to Image Registration

The template layer (source) are registered to the corresponding peak temperature image (target) by estimating a projective transformation between the source template and the target image. The transformation is estimated between the edges of the template and the edges of the initially segmented image using fixed threshold. Given a source shape model $\mathbf{M_s}$ that represents the template layer edges, and a target shape $\mathbf{M_t}$ that represents the initially segmented image edges, a transformation $\mathbf{A}$ that moves points from $\mathbf{M_s}$ to $\mathbf{M_t}$ is needed. The selected transformation has a set of parameters that will be estimated to minimize a certain energy function, similar techniques used before to estimate an affine transformation. Similar to [12], assume that the transformation is a 2D projective and hence it will have the following homogeneous format:

$$\mathbf{A} = \begin{pmatrix} a_1 a_2 a_3 \\ a_4 a_5 a_6 \\ a_7 a_8 a_9 \end{pmatrix} \tag{1}$$

Assume that $x_i \in \mathbf{M_s}, i = 1,2,\ldots,N_s$ and $y_i \in \mathbf{M_t}$ is the closest point to $\mathbf{A}x_i$ on the target shape where N_s is the number of points on the source surface. Note that both $x_i = \begin{pmatrix} x_{i1} \\ x_{i2} \\ 1 \end{pmatrix}$ and $y_i = \begin{pmatrix} y_{i1} \\ y_{i2} \\ 1 \end{pmatrix}$ points are put in the homogeneous vector notation of size 3×1. Consider the Euclidean distance between the moved point and its closes position to be the dissimilarity measure as follows:

$$d_i = ||\mathbf{A}x_i - y_i||. \tag{2}$$

Solving for **A** that minimizes the distance d_i between the two shape models, as shown in [12], will compute the parameters of the required projective transformation. This process is repeated on the transformed shape until the change in the transformed points is not significant. Fig. 4 shows the registration results for samples from the four builds at different layers.

Laser beam power

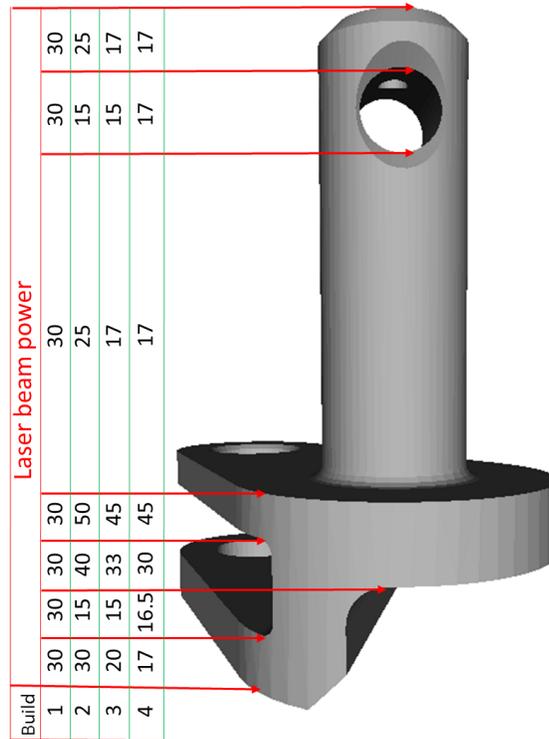| Build							
1	30	30	30	30	30	30	30
2	30	15	40	50	25	15	25
3	20	15	33	45	17	15	17
4	17	16.5	30	45	17	17	17

Figure 3. Laser beam power setting in watts as a function of layer area for the four builds.
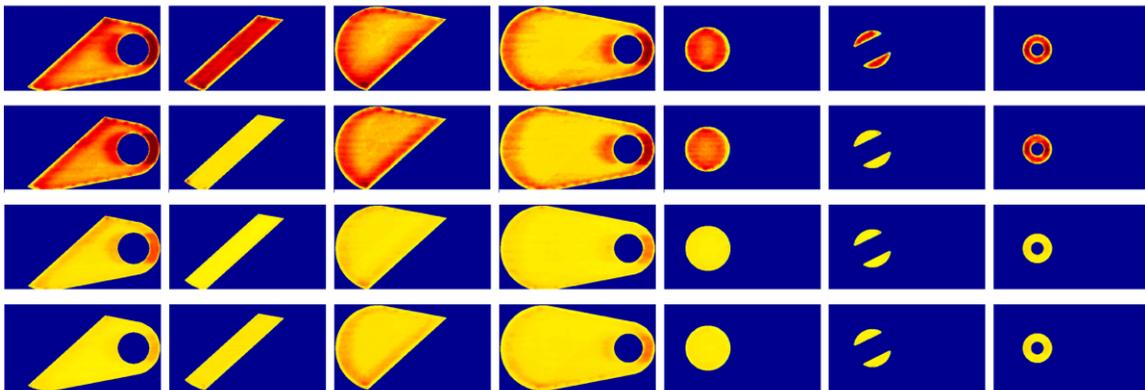
Figure 4. Examples of peak temperature during the scan of different layers. The first row is for the first build as described in figure 3. The effect of changing laser power is very clear in the second row when we reduced the laser power of the small cross-sectional area too much. The last row shows a uniform peak temperature.

Analysis of Results

The system setup is shown in Fig. 2. The system consists of the new "open architecture" LS machine, thermal camera and a 2 in flat gold mirror as described in the data collection section above. Four builds were conducted in the new "open architecture" LS machine. Builds are done using PA 650 nylon 12 laser sintering material [13]. Builds are done in the vertical orintation as shown in Fig. 3. The first build is conducted with fixed laser beam power, while the other three builds are conducted with variable laser beam power as a function of layer cross-sectional area as shown in Fig. 3. Four different videos are recorded during the build of the test parts with four different scan parameters settings.

Thermal data for the builds are segmented using template to image registration method as explained before. Samples of segmented images for every build are shown in Fig. 4. The average peak temperature in every layer is used as a measure. Fig. 5 shows the plots of the average peak temperature versus layer number for the four builds. These plots show the effect of changing the laser power on the average peak temperature. The first plot, for the build with fixed laser power, shows that layers with small area have higher temperature values and the very large area has the lowest temperature. With changing the laser power, as detaild in Fig. 3, we can see how this affect the average peak temperarure in the second, third, and last plot. The results indeed confirmed that we can get a uniform peak temperature as shown in the last plot. This observation has been confirmed by Fig. 6 that shows that the very small area has the highest temperature for the build without control, but with controlling the laser power we get a constant peak teperature for different areas. These results approved that the layer area can be used as a control signal to control the laser beam power to maintain constant peak temperature throughout the part. This produced more consistent part properties.

Discussion

This paper addresses the problem of controlling the 3D printing process. We presented an approach for polymer laser sintering process control based on part geometry. The proposed control system utilized information from layerwise geometry models for the part to control the fabrication process. We used a single layer geometry measure, which is the layer scanned area, to pre adjust the laser beam power for every layer. We empirically adjusted the laser power based on the layer cross-sectional area. Results from four different builds show that we can get a uniform average peak temperature throughout the part. For future work we will use the collected data to estimate a closed form relation between the layer area, the peak temperature, and the laser beam power to precisely control the laser power. Also, we will study the effect of the pre-scan powder bed temperature on the fabrication process.
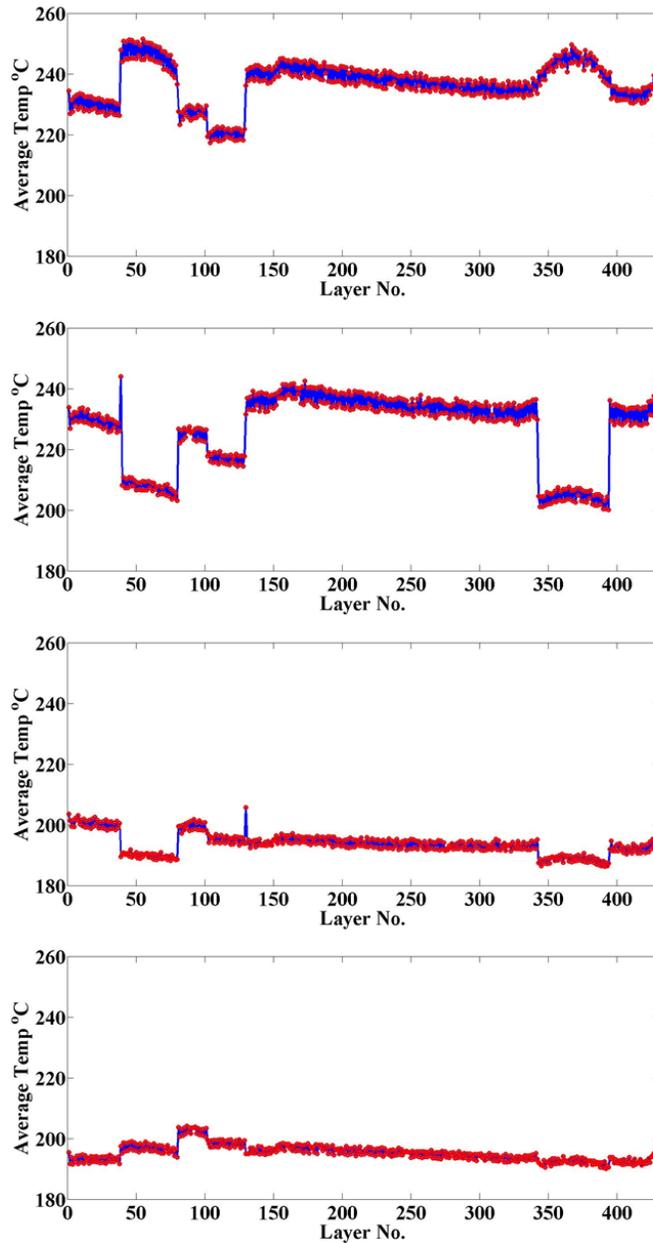
Figure 5. Average peak temperature in every layer depends on the cross-sectional area and the laser beam power. The lower plot for the last build approved that we can get a uniform peak temperature by controlling the laser power.
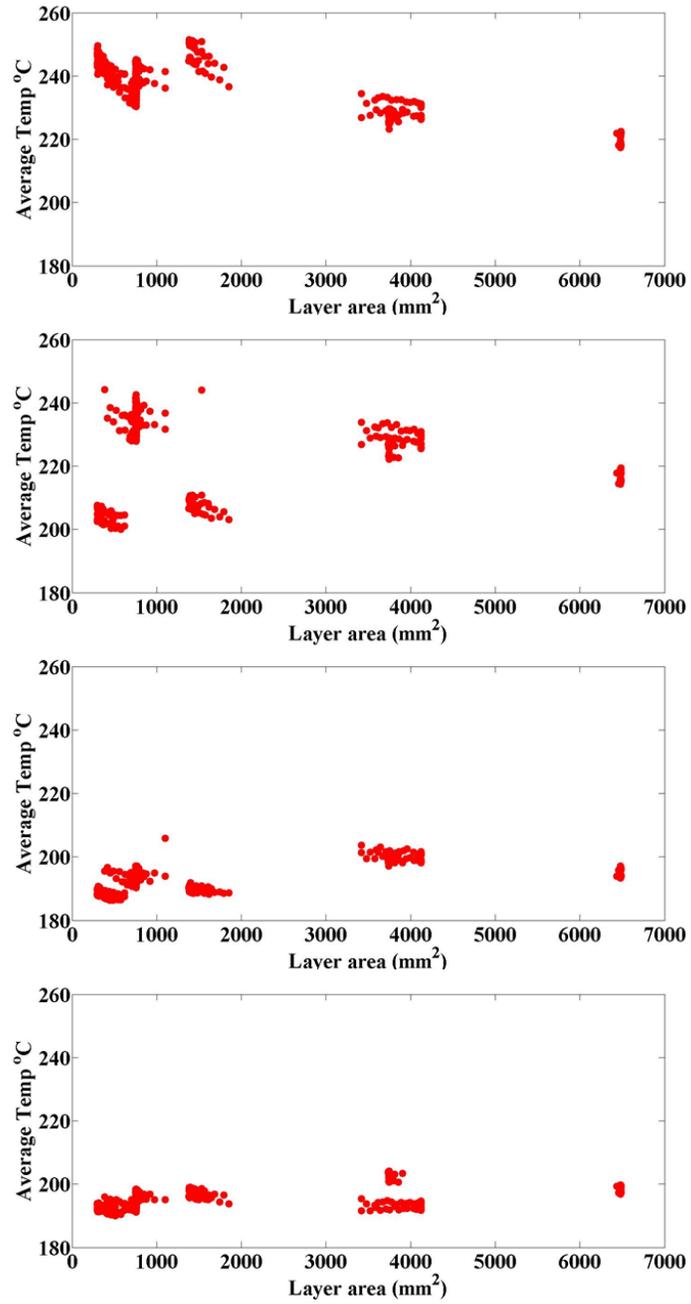
Figure 6. Average peak temperature in every layer versus the cross-sectional area.

References

[1] Ignatiev, M., Smurov, I., and Flamant, G., 1994. "Real-time optical pyrometer in laser machining". *Measurement Science and Technology,*(5), p. 563.

[2] Martinen, D., and Wohlfahrt, H., 1997. "Process monitoring in laser beam cutting on its way to industrial application". *Proc. SPIE, Lasers in Material Processing, 3097*pp. 29–37.

[3] Smurov, I., 2007. "Laser process optical sensing and control". *In IV International WLT-Conference on Lasers in Manufacturing*, pp. 537–546.

[4] Doubenskaia, M., Pavlov, M., and Chivel, Y., 2010. "Optical system for on-line monitoring and temperature control in selective laser melting technology". *Key Engineering Materials,* **437**, pp. 458–461.

[5] Chivel, Y., and Smurov, I., 2010. "On-line temperature monitoring in selective laser sintering/melting". *Physics Procedia,* **5**, pp. 515–521.

[6] Doubenskaia, M., Pavlov, M., Grigoriev, S., Tikhonova, E., and Smurov, I., 2012. "Comprehensive optical monitoring of selective laser melting". *Journal of Laser Micro Nanoengineering 7.3*, pp. 236–243.

[7] Diller, T.; Sreenivasan, R. B. J. B. D. L. J., 2010. "Thermal model of the build environment for polyamide powder selective laser sintering". *Proceedings of the 21st Annual International Solid Freeform Fabrication Symposium (SSF 2010): The University of Texas at Austin*, pp. 539–548.

[8] Wegner, A., and Witt, G., 2011. "Process monitoring in laser sintering using thermal imaging". *Proceedings of the 22nd Annual International Solid Freeform Fabrication Symposium (SFF 2011), The University of Texas at Austin*, pp. 405–414.

[9] Rodriguez, E., Medina, F., Espalin, D., Terrazas, C., Muse, D., and Henry, C., et al 2012. "Integration of a thermal imaging feedback control system in electron beam melting". *Proceedings of the 23rd Annual International Solid Freeform Fabrication Symposium (SFF 2012)), The University of Texas at Austin.* pp. 945–961.

[10] Karnati, S., Matta, N., Sparks, T., and Liou, F., 2013. "Vision-based process monitoring for laser metal deposition processes". *Proceedings of the 24th Annual International Solid Freeform Fabrication Symposium (SFF 2013)), The University of Texas at Austin*.

[11] Schwerdtfeger, J., Singer, R. F., and Körner, C., 2012. "*In situ* flaw detection by ir-imaging during electron beam melting". *Rapid Prototyping Journal,* **18**(4), pp. 259–263.

[12] M. Abdelrahman, T. Starr, "Layerwise monitoring of polymer laser sintering using thermal imaging". *Proceedings of the 25th Annual International Solid Freeform Fabrication Symposium (SFF 2014), The University of Texas at Austin*.

[13] Pa 650, nylon 12 laser sintering material. *http://alm-llc.com/Tech_Data_Sheets/ PA_650.pdf*.

[14] M. Abdelrahman, T. Starr, " Quality Certification and Control of Polymer Laser Sintering: Layerwise Temperature Monitoring Using Thermal Imaging", *The International Journal of Advanced Manufacturing Technology (accepted 2015)*